



A rapid and sensitive colorimetric assay method for Co^{2+} based on the modified Au nanoparticles (NPs): Understanding the involved interactions from experiments and simulations

Yumin Leng^a, Fuqiang Zhang^{a,c}, Yujie Zhang^a, Xiaoqin Fu^b, Yanbo Weng^b, Liang Chen^{a,*}, Aiguo Wu^{a,*}

^a Ningbo Institute of Materials Technology & Engineering (NIMTE), Chinese Academy of Sciences (CAS), Ningbo 315201, China

^b Ningbo Environmental Monitoring Center, Ningbo 315012, China

^c College of Chemistry and Materials Science, Anhui Key Laboratory of Chemo-Biosensing, Anhui Normal University, Wuhu 241000, China

ARTICLE INFO

Article history:

Received 28 November 2011

Received in revised form 20 March 2012

Accepted 22 March 2012

Available online 29 March 2012

Keywords:

Au nanoparticles

2-Thioethanoate

Cobalt ions

Fourier transform infra-red spectroscopy

X-ray photoelectron spectroscopy

Density functional theory calculation

ABSTRACT

We previously reported a colorimetric assay method for Co^{2+} based on the thioglycolic acid (TGA) functionalized hexadecyl trimethyl ammonium bromide (CTAB) modified Au NPs. However, the detection limit of 3×10^{-7} M was still higher than that of the sanitary standard for drinking water (6.8×10^{-8} M). In addition, the interactions between the modifier and Au NPs, and between the modifier-Au NPs and Co^{2+} remain to be clarified and confirmed. Thus, in the present study, the modified Au NPs solution was dialyzed and its detection limit was optimized to be 5×10^{-10} M. The interactions between the modifier and Au NPs, and between the modifier-Au NPs and Co^{2+} were investigated in both experimental characterizations and theoretical calculations, consistently confirming that the Au NPs were modified by the negatively charged anions of $[\text{SCH}_2\text{CO}_2]^{2-}$ through Au–S bonds and Co^{2+} was recognized by the modifier-Au NPs through Co–O chelate bonds. The results of X-ray photoelectron spectroscopy (XPS) suggest that there were no chemical bonds formed between CTAB and Co^{2+} . Moreover, the colorimetric assay of Co^{2+} using the modified Au NPs has been proved to be a rapid, very sensitive and highly selective method. The validation of the method was carried out by analysis of a certified reference material, GSBZ 50030-94.

© 2012 Elsevier B.V. All rights reserved.

1. Introduction

Cobalt is one of the essential trace elements that humans and many other living creatures require for good health [1]. As part of Vitamin B12, cobalt can promote the formation of red blood cells [2]. However, cobalt also causes severe effects on human beings and animals arising from overexposure to the environmental water polluted by Co^{2+} [3–5]. The toxicological effects of Co^{2+} on human beings may lead to loss of appetite, flushing and vasodilatation, even terrible diseases such as anemia and cardiomyopathy [6,7]. Thus, the determination of trace amount of Co^{2+} in biological and environmental samples is very essential. Several methods have been used for Co^{2+} analysis, including inductively coupled plasma–atomic emission spectrometry (ICP–AES) [8], fluorescence techniques [9], fiber optic–linear array detection spectrophotometry (FO–LADS) [10], electrochemical approach [11,12], flame atomic absorption spectrometry (FAAS) [4,5,13] and spectrophotometry [14], etc. Without the aid of any advanced instruments, colorimetric methods can be convenient and easily monitored with the naked eyes. So the colorimetric methods have attracted considerable

attention in detection of toxic metal ions including Co^{2+} [15–19]. Yao et al. [15] and Maity and Govindaraju [16] applied the different colorimetric assay methods for Co^{2+} with the detection limit of 1×10^{-5} M and 1×10^{-6} M, respectively. Previously, we developed a colorimetric assay method for Co^{2+} based on the thioglycolic acid (TGA) functionalized hexadecyl trimethyl ammonium bromide (CTAB) modified Au NPs with the detection limit of 3×10^{-7} M [19]. All the reported limits of colorimetric detection of Co^{2+} are quite higher than the level of 6.8×10^{-8} M according to the sanitary standard for drinking water [21]. As a result, there is high demand for the development of highly sensitive methods to detect Co^{2+} . Moreover, up to date, all the researches on the interactions between the ligands and the detected ions/biological molecules still built on assumptions and conjecture [15–20].

Here, we developed a highly rapid and sensitive colorimetric assay method for Co^{2+} based on dialyzing the previous modified Au NPs solution [19] and its limit of colorimetric detection was optimized to be 5×10^{-10} M, which is much lower than previously reported data of 3×10^{-7} M [19] and even lower than the level of 6.8×10^{-8} M according to the sanitary standard for drinking water [21]. In addition, we extend our effort to investigate the interactions between the modifier and Au NPs, and between the modifier-Au NPs and Co^{2+} using the experimental means and density functional theory (DFT) calculations. Experimentally, dynamic

* Corresponding authors. Tel.: +86 574 86685039, fax: +86 574 86685163.

E-mail addresses: chenliang@nimte.ac.cn (L. Chen), aiguo@nimte.ac.cn (A. Wu).

light scattering (DLS) has been proved to be a powerful tool for determining small changes in the size and zeta potential of particles in solutions [22–24]. Moreover, DLS has been demonstrated to be sensitive in probing the interaction between molecules and Au NPs [22–24]. Herein, DLS was used to determine the changes both in the size and zeta potential of the Au NPs modified by 2-thioethanoate ($[\text{SCH}_2\text{CO}_2]^{2-}$), which were dissociated from TGA ($\text{HSCH}_2\text{CO}_2\text{H}$) in solution. Theoretically, the DFT calculation has proved to be a powerful tool for determining the structures and interaction mechanisms of molecules [25–28]. In particular, the DFT calculation has been used to explore the vibrational frequencies of molecules [25,26]. In the current work, the DFT calculations were used to determine the molecular structures of $[\text{AuSCH}_2\text{CO}_2]^-$ and $[\text{3AuSCH}_2\text{CO}_2 + \text{Co}]^-$ involved in the experiment, and simulate their vibrational frequencies compared with the experimental results. The corresponding vibrational spectra of Fourier transform infra-red spectroscopy (FT-IR) and DFT calculations consistently confirmed that the Au NPs were modified by $[\text{SCH}_2\text{CO}_2]^{2-}$ through Au-S bonds and Co^{2+} was recognized by the modifier-Au NPs through Co–O bonds, which were proved by XPS to be Co–O chelate bonds. The combination of experimental characterizations and theoretical calculations demonstrated the hypothetical mechanism in our previous work [19]. While there were no chemical bonds formed between CTAB and Co^{2+} .

In addition, the recognition time of Co^{2+} by modified Au NPs has been proved to be within 1 min, which is much less than the detection time (~ 3 h) of ICP-AES needed for the pre-concentration of trace Co^{2+} before analysis. The probe of modified Au NPs has very high specificity toward Co^{2+} both in freshwater and hypothetical seawater. The practicality of the modified Au NPs for analysis of Co^{2+} in real environmental water was demonstrated by the colorimetric assay with satisfactory results.

2. Experimental

2.1. Materials

Thioglycolic acid (TGA), LiCl, $\text{MgCl}_2 \cdot 6\text{H}_2\text{O}$, $\text{FeCl}_2 \cdot 4\text{H}_2\text{O}$, $\text{BaCl}_2 \cdot 2\text{H}_2\text{O}$ and $\text{CuSO}_4 \cdot 5\text{H}_2\text{O}$ were obtained from Aladdin-regent Co. Ltd (Shanghai, China). Sodium borohydride (NaBH_4), chloroauric acid tetrahydrate ($\text{HAuCl}_4 \cdot 4\text{H}_2\text{O}$), KCl, NaCl, AlCl_3 , FeCl_3 , ZnCl_2 , HgCl_2 , $\text{CrCl}_3 \cdot 6\text{H}_2\text{O}$, $\text{CoCl}_2 \cdot 6\text{H}_2\text{O}$, $\text{SrCl}_2 \cdot 6\text{H}_2\text{O}$, $\text{NiCl}_2 \cdot 6\text{H}_2\text{O}$, $\text{MnCl}_2 \cdot 4\text{H}_2\text{O}$, $\text{CdCl}_2 \cdot 2.5\text{H}_2\text{O}$, CaCl_2 , $\text{K}_2\text{Cr}_2\text{O}_7$, Na_2CO_3 , Na_3PO_4 , Na_2SO_4 , $\text{Na}_2\text{C}_2\text{O}_4$, $\text{Pb}(\text{NO}_3)_2$, lysine, threonine, cysteine, arginine, histidine and hexadecyl trimethyl ammonium bromide (CTAB) were obtained from Sinopharm Chemical Reagent Co., Ltd (Beijing, China). The certified reference material GSBZ 50030-94 was obtained from Institute for Environmental Reference Materials of Ministry of Environmental Protection (Beijing, China). All of the chemicals were used without purification. Millipore-Q water was used throughout the experiment. All glassware were washed with aqua regia ($\text{HCl}/\text{HNO}_3 = 3:1$ (v/v). It is very strong corrosive!!!) and then cleaned with Milli-Q water.

2.2. Methods and characterization

X-ray powder diffraction (XRD) was performed using a Bruker D8 Advance/Discover diffractometer (Bruker Co. Ltd., Germany) with Cu $\text{K}\alpha$ radiation ($\lambda = 1.5406 \text{ \AA}$). Fourier transform infra-red spectroscopy (FT-IR) was performed using a Nicolet 6700 spectrometer. Dynamic light scattering (DLS) was performed using Zetasizer Nano ZS instrumentation (Malvern Instruments Ltd). Transmission electron microscopy (TEM) and energy dispersive X-ray spectroscopy (EDS) were performed using a Tencai F20 instrument and operated at 200 kV. UV–vis absorption spectra were

recorded in the range of 400–800 nm using a Lambda 950 UV–vis spectrophotometer from Perkin Elmer. X-ray photoelectron spectroscopy (XPS) was performed using an AXIS Ultra DLD instrument with Mg $\text{K}\alpha$ radiation as the X-ray source. The including inductively coupled plasma–atomic emission spectrometry (ICP-AES) data were recorded on an Optima 2100DV ICP instrument.

2.2.1. Preparation of the modified Au NPs

According to Murphy's method [29], Au NPs were prepared by reducing HAuCl_4 with NaBH_4 , and stabilized by CTAB. The synthetic Au NPs solution was centrifuged to remove CTAB and characterized by XRD. 100 μL of TGA ($\text{HSCH}_2\text{CO}_2\text{H}$) was added into 100 mL of the Au NPs solution without centrifugation, while the pH value of the mixed solution was controlled to be 8.0. The concentrations of TGA and Au NPs in the solution were controlled to be $\sim 1.3 \times 10^{-2} \text{ M}$ and $2.1 \times 10^{-4} \text{ M}$, respectively. After adding TGA for 0 min, 5 min, 20 min, 40 min, 60 min, 90 min, 120 min and 150 min, 12 mL of the mixed solution was centrifuged at 10,000 rpm for 10 min and characterized the particle size and zeta potential of the modified Au NPs using DLS, respectively. The modified Au NPs were then characterized by TEM and EDS.

2.2.2. Interference studies

The selective recognition of Co^{2+} by modified Au NPs in freshwater and hypothetical seawater was studied respectively. The selectivity for Co^{2+} in freshwater was investigated as follows: the representative metallic ions (Li^+ , Na^+ , K^+ , Mg^{2+} , Ca^{2+} , Sr^{2+} , Ba^{2+} , Mn^{2+} , Fe^{2+} , Fe^{3+} , Al^{3+} , Ni^{2+} , Cu^{2+} , Zn^{2+} , Cd^{2+} , Cr^{3+} , $\text{Cr}(\text{VI})$, Hg^{2+} , Pb^{2+} , Co^{2+}) (0.5 mL , $8 \times 10^{-5} \text{ M}$), anions (Cl^- , $\text{C}_2\text{O}_4^{2-}$, SO_4^{2-} , CO_3^{2-} , PO_4^{3-}) (0.5 mL , $8 \times 10^{-4} \text{ M}$) and amino acids (lysine, threonine, cysteine, arginine, histidine) (0.5 mL , $8 \times 10^{-5} \text{ M}$) were added into the modified Au NPs solutions (3.5 mL), respectively. Their color and UV–vis spectra were compared with the blank control group. The final concentrations of the tested metallic ions, anions and amino acids were 10^{-5} M , 10^{-4} M and 10^{-5} M , respectively.

The procedure for the selective recognition of Co^{2+} by modified Au NPs in hypothetical seawater is similar with that in freshwater, while the significant difference is that the NaCl concentration in hypothetical seawater was controlled to be 0.62 M, which is the highest concentration of NaCl in seawater.

2.2.3. The detection of Co^{2+} by modified Au NPs

For the detection of Co^{2+} , the modified Au NPs solutions ($\sim 2.1 \times 10^{-4} \text{ M}$) was dialyzed to remove the excess CTAB and TGA, and then mixed with the various concentrations of Co^{2+} ranging from 0 to $1 \times 10^{-4} \text{ M}$.

To probe the interactions between the modifier-Au NPs and Co^{2+} , 10 mL of different concentrations of Co^{2+} (0 , 2×10^{-4} and $2 \times 10^{-3} \text{ M}$) were added to 30 mL of the modifier-Au NPs solutions, respectively. The final concentrations of Co^{2+} in the modifier-Au NPs solutions were 0 , 5×10^{-5} and $5 \times 10^{-4} \text{ M}$, respectively. The mixtures without centrifugation were freeze-dried for 36 h and characterized by FT-IR and XPS.

2.3. Structure and frequency calculations

The geometry optimizations on the structures of $[\text{AuSCH}_2\text{CO}_2]^-$ and $[\text{SCH}_2\text{CO}_2]^{2-}$ were performed by means of DFT methods using the GAUSSIAN03 quantum chemistry package. The stable conformer of $[\text{3AuSCH}_2\text{CO}_2 + \text{Co}]^-$ was determined by optimizing the trial structures (~ 1000) obtained by adding Co^{2+} to the stable conformers of $[\text{AuSCH}_2\text{CO}_2]^-$ at different binding sites. In order to ascertain the structural accuracy and stability, the vibrational frequencies of the stable structures of $[\text{AuSCH}_2\text{CO}_2]^-$, $[\text{SCH}_2\text{CO}_2]^{2-}$ and $[\text{3AuSCH}_2\text{CO}_2 + \text{Co}]^-$ were calculated at the BHandHLYP/6-31G* level and compared with the experimental FT-IR spectra. We

adopted the BHandHLP level of theory [27], and the 6-31G* basis set [30] for O, C, H, and S atoms and the LANL2DZ (Los Alamos National Laboratory 2 double ξ) basis set [31] for Au and Co atoms.

3. Results and discussion

3.1. The characterization of the modified Au NPs

The synthetic Au NPs were determined by XRD to have a face-centered cubic (fcc) crystalline structure. Thus, the fcc structure of the possible cell unit of Au₁₄ cluster was modeled in this study at the bhandhlyp/LANL2DZ level. The Au–Au distance was calculated to be about 2.8 Å within the range of 2.68–3.12 Å [32,33]. The XRD pattern of Au NPs and the fcc structure of Au₁₄ cluster are shown in Fig. S1 (Supporting information part).

In our experiment, TGA (HSCH₂CO₂H) in alkaline solution dissociated into H⁺ ions and the negatively charged anions of [SCH₂CO₂]²⁻, which were proposed to partly modify the surface of Au NPs through the Au–S bonds. So the structures of [AuSCH₂CO₂]⁻ and [SCH₂CO₂]²⁻ were modeled and determined by performing theoretical calculations. The Cartesian coordinates of the optimized structures of [AuSCH₂CO₂]⁻ and [SCH₂CO₂]²⁻ are given in Supporting information (Table S1). The calculated Au–S distance of 2.35 Å is similar to the reported value of 2.30 Å [32]. The vibrational frequencies of the obtained structures of [SCH₂CO₂]²⁻ and [AuSCH₂CO₂]⁻ were simulated by DFT calculations and shown in Fig. 1 (green and blue curves), which also shows the merged frequencies of the two structures (red curve) and the FT-IR spectra (black curve) of the negatively charged anions of [AuSCH₂CO₂]⁻ and [SCH₂CO₂]²⁻. The characteristic bands of the simulated IR spectra of the [AuSCH₂CO₂]⁻ and [SCH₂CO₂]²⁻ structures are in good agreement with the experiments within the region of 250–700 cm⁻¹. The Au NPs modified by [SCH₂CO₂]²⁻ have been confirmed from the simulated and experimental Au–S stretching vibration around 278.5 cm⁻¹.

As shown in Fig. 2, the process of [SCH₂CO₂]²⁻ modified Au NPs was characterized by DLS, which determined the changes both in the size and zeta potential of the hydrated Au NPs as function of the modified time within 150 min. The particle size of the hydrated Au NPs increased exponentially as the modified time increased (see Fig. 2a). The zeta potential of the hydrated Au NPs decreased exponentially as the Au NPs were gradually modified by the negatively charged anions of [SCH₂CO₂]²⁻ (see Fig. 2b). The exponential increase in the size and decrease in the zeta potential of the hydrated Au NPs with the modified time both suggested that the Au NPs were successfully modified by [SCH₂CO₂]²⁻ in 40 min. The TEM and EDS images of the modified Au NPs are shown in

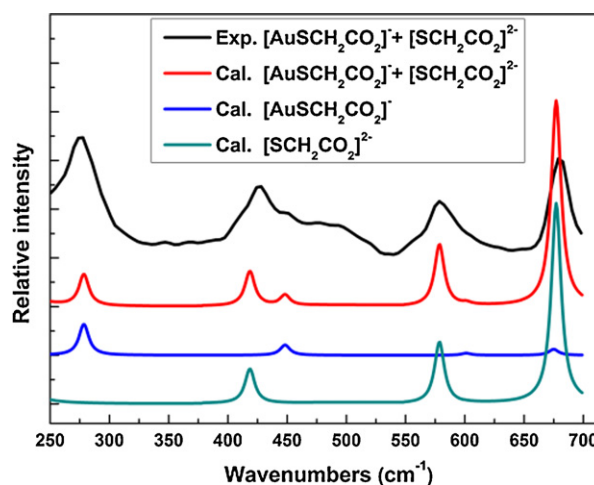


Fig. 1. Comparison of the experimental and simulated IR spectra of [AuSCH₂CO₂]⁻ and [SCH₂CO₂]²⁻ in the region of 250–700 cm⁻¹. (For interpretation of the references to color in the sentence, the reader is referred to the web version of the article.)

Supporting Information (Fig. S2a). The dispersed and modified Au NPs with an average diameter of 28.5 nm can be seen from the TEM image in Fig. S2a. The modified Au NPs with the characteristic elements gold (Au), sulfur (S) and oxygen (O) can be seen from the EDS spectrum image in Fig. S2a.

3.2. Rapid recognition of Co²⁺ by modified Au NPs

To address the recognition time of Co²⁺ by modified Au NPs, 1 × 10⁻⁶ M of Co²⁺ was added to the modified Au NPs solution with dialysis, the changes of its UV–vis spectra were recorded within 30 min and the ratio of absorption at 462 nm and 527 nm was considered here. As shown in Fig. 3, the sharp change in the absorption ratio after addition of Co²⁺ within 1 min proved that the recognition of Co²⁺ by modified Au NPs was highly rapid.

3.3. Sensitive recognition of Co²⁺ by modified Au NPs

To evaluate the detectable minimum concentration of Co²⁺, various concentrations of Co²⁺ ranging from 0 to 1 × 10⁻⁴ M were added into the modified Au NPs solution with dialysis. As shown in Fig. 4a, the color change could be immediately observed when the concentration of Co²⁺ is beyond 5 × 10⁻¹⁰ M.

Fig. 4b shows the absorption spectra of the modified Au NPs solution with different concentrations of Co²⁺. The absorption peak is clearly blue-shifted and its intensity increases with the increase

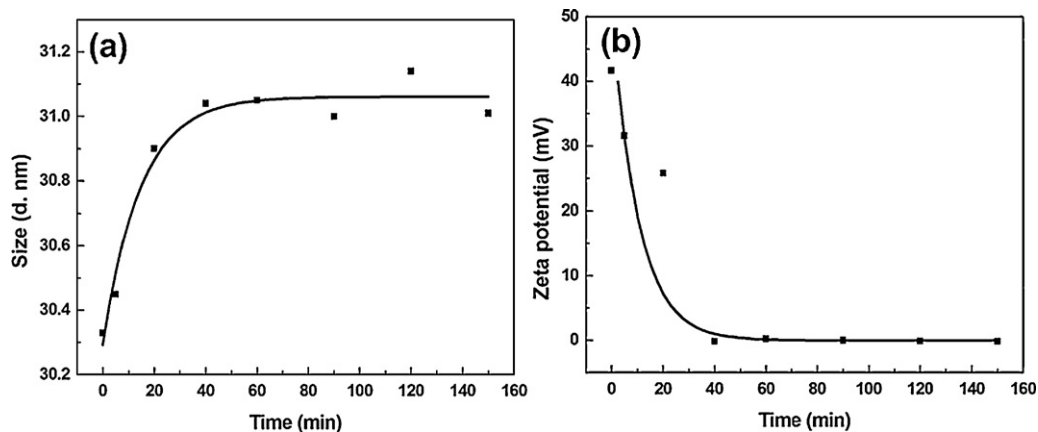


Fig. 2. The changes in the size and zeta potential of the hydrated Au NPs as function of the time of Au NPs modified by [SCH₂CO₂]²⁻.

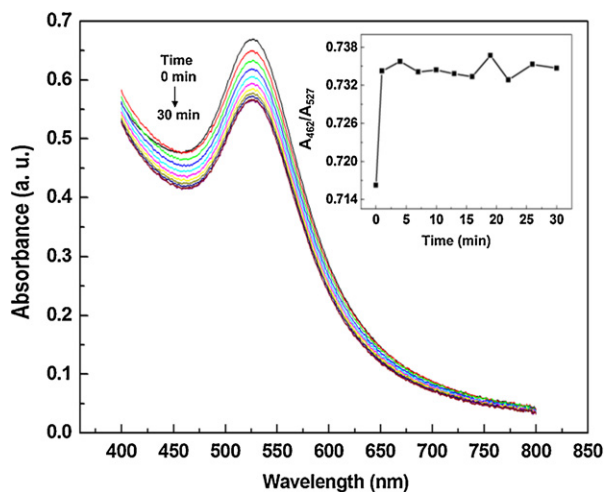


Fig. 3. UV-visible spectra of the modified Au NPs solution after the addition of 1×10^{-6} M Co^{2+} within 30 min. Inset: absorption ratios (462 over 527 nm) as function of the reaction time.

of Co^{2+} concentration, due to the Co–O chelate bonds formed between the modifier–Au NPs and Co^{2+} . The ratio (A/A_0) of the absorption peak intensity of the modified Au NPs with Co^{2+} over that without Co^{2+} , was used to express the molar ratio of aggregated to dispersed Au NPs. The ratio (A/A_0) as a function of Co^{2+} concentration is shown in the inset of Fig. 4b. The linear relationship ($R^2 = 0.995$) can be inferred, manifesting the dynamic range from 0 to 5 nM and a limit of detection (LOD) being 4.65×10^{-10} M (see the calculation method in the Supporting information). The detection limits of the colorimetric assay and calculation for Co^{2+} were 5×10^{-10} M and 4.65×10^{-10} M respectively, both of which are quite lower than the previously reported data of 3×10^{-7} M [19] and even lower than the sanitary standard (6.8×10^{-8} M) for drinking water [21]. The recognition of Co^{2+} by modified Au NPs was highly sensitive. Moreover, the modified Au NPs solution with dialysis is highly stable. After 10 months of storage, the modified Au NPs solution with dialysis has very high specificity toward Co^{2+} (See the bottom image in Fig. S3 in Supporting information).

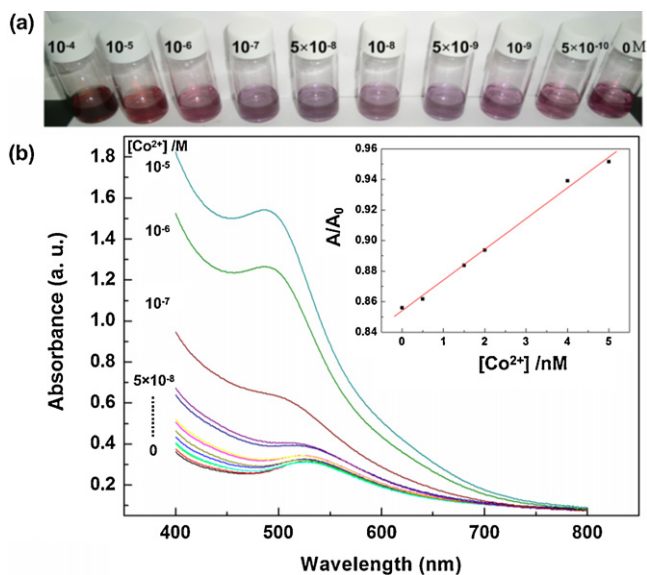


Fig. 4. Photographs and UV-visible spectra of the modified Au NPs solutions with various concentrations of Co^{2+} . Inset: absorption rates (A/A_0) as a function of Co^{2+} concentrations (the concentrations of Co^{2+} were 0 , 5×10^{-10} , 1.5×10^{-9} , 2×10^{-9} , 4×10^{-9} , 5×10^{-9} , 7×10^{-9} , 10^{-8} , 2×10^{-8} , 5×10^{-8} , 10^{-7} , 10^{-6} , 10^{-5} and 10^{-4} M).

3.4. Selective recognition of Co^{2+} by modified Au NPs

The selective recognition of Co^{2+} by modified Au NPs in freshwater and hypothetical seawater was investigated by considering other 19 metallic ions (Li^+ , Na^+ , K^+ , Mg^{2+} , Ca^{2+} , Sr^{2+} , Ba^{2+} , Mn^{2+} , Fe^{2+} , Fe^{3+} , Al^{3+} , Ni^{2+} , Cu^{2+} , Zn^{2+} , Cd^{2+} , Cr^{3+} , Cr(VI) , Hg^{2+} , and Pb^{2+}), 5 anions (Cl^- , $\text{C}_2\text{O}_4^{2-}$, SO_4^{2-} , CO_3^{2-} , PO_4^{3-}) and 5 amino acids (lysine, threonine, cysteine, arginine, histidine). The concentrations of the above-mentioned metallic ions, anions and amino acids in the modified Au NPs solutions were 10^{-5} M, 10^{-4} M and 10^{-5} M, respectively. The corresponding photo images and UV-vis spectra are shown in Fig. 5. It is clear that the probe of modified Au NPs has very high specificity toward Co^{2+} both in freshwater (see Fig. 5a/c) and hypothetical seawater (see Fig. 5b/d). The reason for the perfect selectivity of Co^{2+} against other metallic ions, should be the metal ion affinity of the modified Au NPs with Co^{2+} relatively higher than with other metallic ions in the experimental condition designed, referring to the calculation data for the oxytocin-metal ions interactions [27]. Thus, when the above-mentioned metal ions coexist, the modified Au NPs would be preferentially interacted with Co^{2+} .

3.5. Characterization for the interactions of the modifier–Au NPs with Co^{2+}

3.5.1. XPS

To investigate the interactions between the modifier–Au NPs (with the component of $[\text{AuSCH}_2\text{CO}_2]^-$) and Co^{2+} , the solutions of CTAB-stabilized ($\text{C}_{16}\text{H}_{33}(\text{CH}_3)_3\text{NBr}$) modifier–Au NPs with different concentrations of Co^{2+} (0 , 5×10^{-5} and 5×10^{-4} M) were freeze-dried for 36 h and characterized by XPS, respectively. The atomic concentrations of Co^{2+} in the three samples of the freeze-dried powers were measured by XPS to be about 0, 0.09% and 0.11%, respectively. The Au 4f, S 2p, C 1s, N 1s, Br 3d, O 1s and Co 2p XPS spectra recorded on the three samples are shown in Fig. 6. The spectra of the Au 4f component show that Au $4f_{7/2}$ core peak at a binding energy of 83.9 eV, and Au $4f_{5/2}$ at 87.5 eV with a difference of 3.6 eV (see Fig. 6 – Au 4f), which are in good agreement with the reported data [34]. As shown in Fig. 6 – S 2p, C 1s, N 1s and Br 3d, the corresponding binding energies of S 2p, C 1s, N 1s and Br 3d components are 163.5 eV, 284.9 eV, 402.0 eV and 67.5 eV, and assigned to S–C, C–C, N–C and Br–N bonds [34,35], respectively. The binding energies of C 1s, N 1s and Br 3d didn't change after adding Co^{2+} , which confirmed that there were no chelate bonds formed between CTAB and Co^{2+} .

The spectra of the O 1s component in the modifier of $[\text{SCH}_2\text{CO}_2]^{2-}$ (the red curve shown in Fig. 6 – O 1s) shows the core peak at 532.4 eV, which can be assigned to C=O group [35]. This peak disappeared and two new peaks appeared at 531.3 eV and 534.5 eV (see the yellow and pink curves in Fig. 6 – O 1s) after the modifier–Au NPs reacted with 0.09% or 0.11% Co^{2+} , indicating that the C=O bonds disappear and the corresponding Co–O and C–O bonds are present due to the interaction between the modifier–Au NPs and Co^{2+} [35].

As shown in Fig. 6 – Co 2p, the difference of binding energies of Co $2p_{3/2}$ and Co $2p_{1/2}$ is 15.2 eV, which is consistent with the reported value of the CoO crystal [34]. While the Co $2p_{3/2}$ core peak at a binding energy of 779.5 eV is lower by 0.9 eV than that of Co $2p_{3/2}$ in the CoO crystal, confirming the formation of Co–O chelate bonds rather than Co–O covalent bonds [34].

3.5.2. FT-IR and simulated

Further, the interactions between the modified Au NPs and Co^{2+} could be confirmed from analysis of the simulated and experimental IR spectra. Computationally, for conformational explorations, the structure of $[\text{3AuSCH}_2\text{CO}_2 + \text{Co}]^-$ (shown in Fig. 7) was obtained

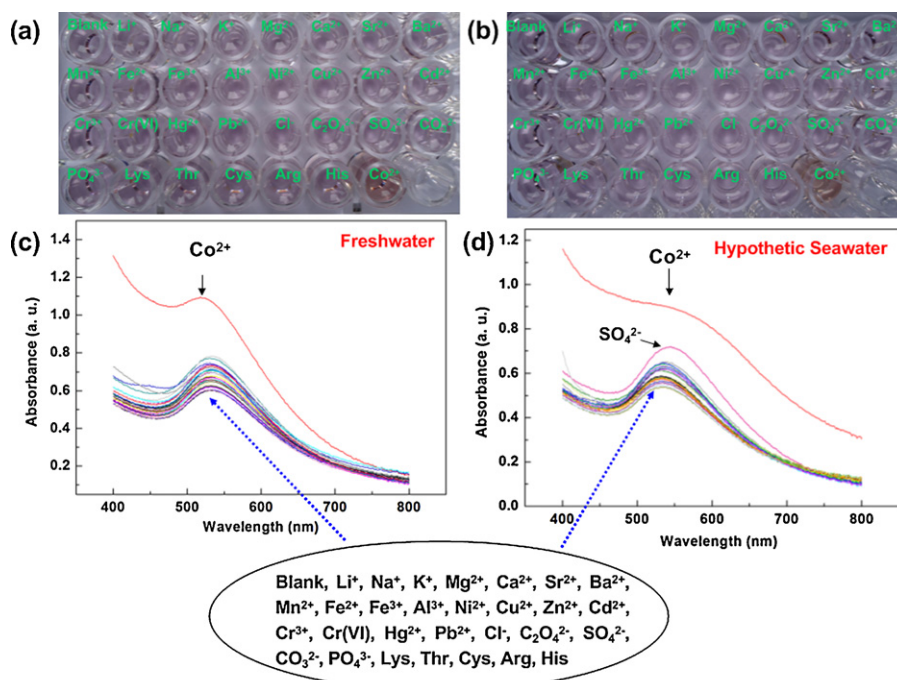


Fig. 5. Color photographs and UV-visible spectra of the modified Au NPs solutions with representative 20 metallic ions, 5 anions and 5 amino acids contained in freshwater and hypothetical seawater, respectively. The concentrations of the metallic ions, anions and amino acids were 10^{-5} M, 10^{-4} M and 10^{-5} M, respectively. The content of NaCl in the hypothetical seawater is 0.62 M.

by extensive DFT calculations for the probable complexes of $[AuSCH_2CO_2]^-$ and Co^{2+} . The vibrational frequencies of the identified stable $[3AuSCH_2CO_2 + Co]^-$ structure were then calculated. Experimentally, the complexes of modified Au NPs with 0, 0.09% or 0.11% Co^{2+} were characterized by FT-IR spectroscopy, respectively.

As shown in Fig. 7, the structure of $[3AuSCH_2CO_2 + Co]^-$ contains a distorted octahedral coordination geometry of CoO, which is similar to the cubic unit cell of CoO crystal [36]. The Cartesian

coordinates of the structure of $[3AuSCH_2CO_2 + Co]^-$ are given in the Supporting Information (Table S2).

The calculated spectrum of the structure of $[3AuSCH_2CO_2 + Co]^-$ and experimental IR spectra are shown in Fig. 8. The symmetrical stretching of O=C=O groups on the structure of $[3AuSCH_2CO_2 + Co]^-$ is observed at the frequency 1581 cm^{-1} , which is well reproduced by the experimental IR spectra. The Co–O stretching is observed at the frequencies 470 cm^{-1} , 498 cm^{-1} and

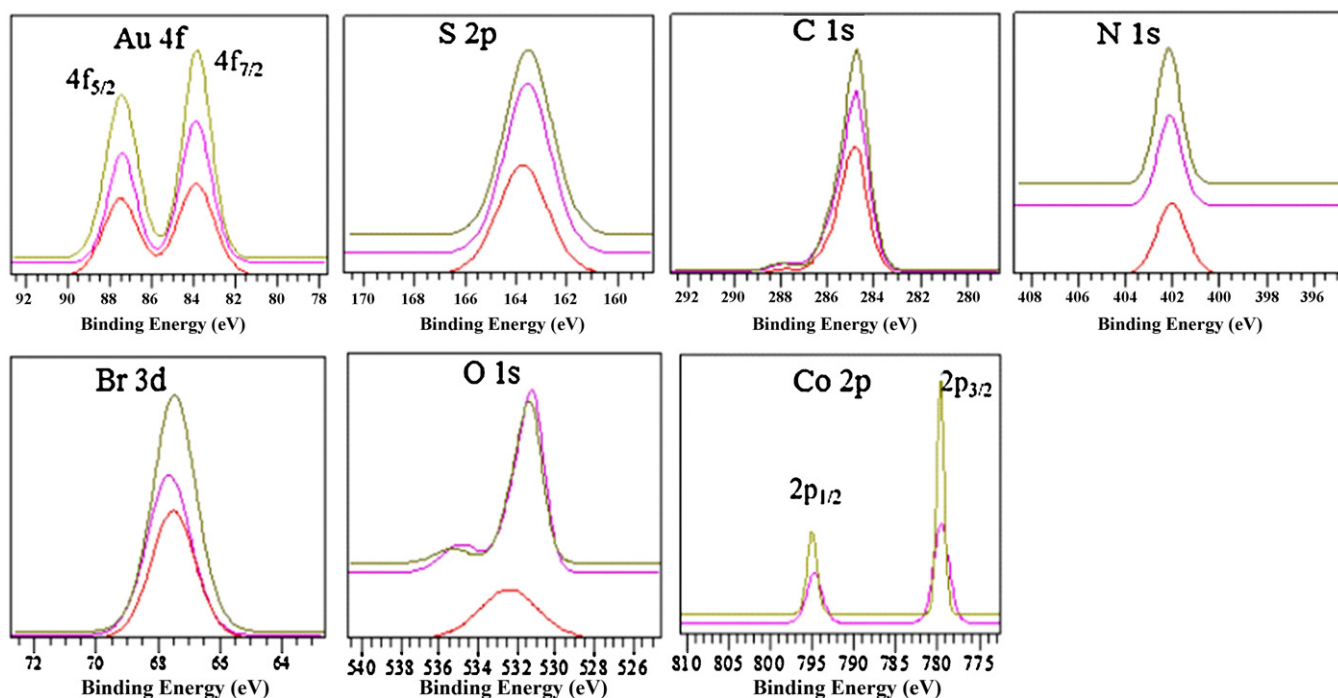


Fig. 6. Comparison of the Au 4f, S 2p, C 1s, N 1s, Br 3d, O 1s and Co 2p spectra recorded on the complexes of the modified Au NPs with 0 (red), 0.09% (yellow) or 0.11% (pink) Co^{2+} . (For interpretation of the references to color in this figure legend, the reader is referred to the web version of the article.)

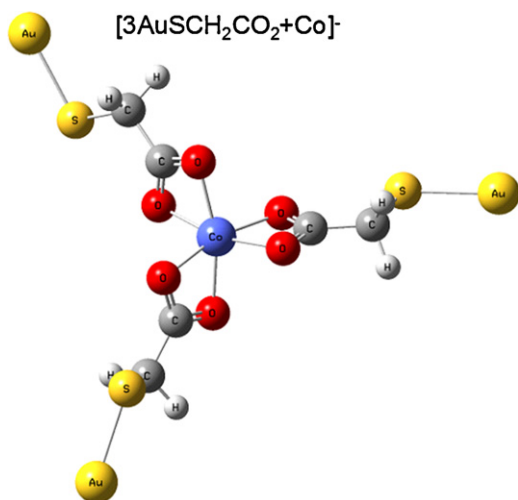


Fig. 7. The optimized structure of $[3\text{AuSCH}_2\text{CO}_2 + \text{Co}]^-$.

542 cm^{-1} in the calculated spectrum. In the experimental IR spectra, as the content of Co^{2+} in the modified Au NPs power increased, the new bands of Co–O stretching also emerged in the range from 400 cm^{-1} to 600 cm^{-1} , in which the band of Co–O stretching at 470 cm^{-1} is in good agreement with the reported value [37]. Some of the bands that appeared around the frequencies 700 cm^{-1} , 950 cm^{-1} and 1450 cm^{-1} were caused by the vibrations of intramolecular bonds in the CTAB molecules (see the FT-IR spectrum of CTAB shown in Fig. S4 in Supporting information). The experimental and simulated results confirmed the formation of Co–O chelate bonds, which is the reason for Co^{2+} -induced aggregation of the modified Au NPs (see Fig. S2b in Supporting information).

3.6. Analysis of reference material

In order to assess the accuracy and validity of the developed procedure, the method was applied to the determination of Co(II) in a certified reference material, GSBZ 50030-94. It was found that analytical result was in good agreement with the certified value (see Table 1).

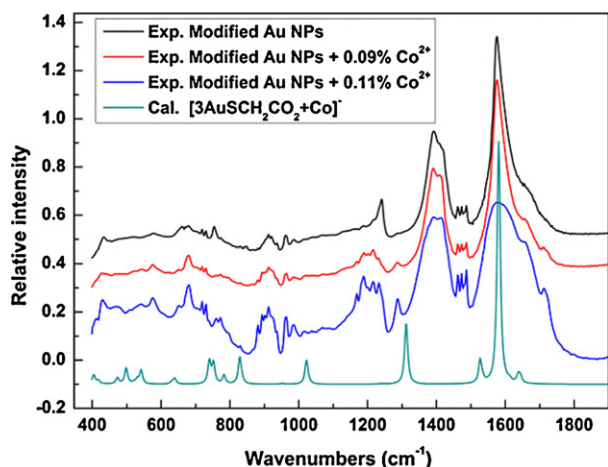


Fig. 8. Experimental IR spectra of the modified Au NPs with 0 (black), 0.09% (red) or 0.11% (blue) Co^{2+} . Simulated IR spectrum of the structure of $[3\text{AuSCH}_2\text{CO}_2 + \text{Co}]^-$ is shown as the lower trace (green). (For interpretation of the references to color in this figure legend, the reader is referred to the web version of the article.)

Table 1

Determination of Co(II) in certified reference material using the developed procedure.

Sample	[Co(II)] (mg/L)	
	Found ^a	Certified
GSBZ 50030-94	0.136 ± 0.01	0.141 ± 0.013

^a Mean \pm standard deviation, $n = 3$.

4. Conclusions

The negatively charged anions of $[\text{SCH}_2\text{CO}_2]^{2-}$ modified Au NPs have been proved to be highly rapid, selective and sensitive for the colorimetric detection of Co^{2+} . The recognition time was very rapid within 1 min and the limit of colorimetric detection of Co^{2+} by modified Au NPs was $5 \times 10^{-10}\text{ M}$, which are much better than the detection time ($\sim 3\text{ h}$) of ICP-AES and the sanitary standard ($6.8 \times 10^{-8}\text{ M}$) for drinking water, respectively.

The interactions involved in the colorimetric detection of Co^{2+} using the modified Au NPs were investigated by both experimental and theoretical methods. The structures of the negative charge components of $[\text{AuSCH}_2\text{CO}_2]^-$, $[\text{SCH}_2\text{CO}_2]^{2-}$ and $[3\text{AuSCH}_2\text{CO}_2 + \text{Co}]^-$ involved in the experiment were determined by DFT calculations. The characteristic bands of the simulated IR spectra of the optimized structures are well produced in the experiments. The simulated and experimental data for Au–S and Co–O stretching vibrations are the strong evidence to prove the Au NPs modified by $[\text{SCH}_2\text{CO}_2]^{2-}$ and the Co–O chelate bonds formed between the modifier–Au NPs and Co^{2+} , respectively. Moreover, the XPS results indicated that there were no chelate bonds formed between CTAB and Co^{2+} .

In addition, the analysis result of Co(II) with the certified value shows the reliability and accuracy of the developed procedure.

Acknowledgments

This work was supported by the Program of Zhejiang Provincial Natural Science Foundation of China under Grant No. R5110230, Natural Science Foundation of China under Grant Nos: 31170964, 31128007, and 51102251, Hundred Talents Program of Chinese Academy of Sciences, and program of Bureau of Academy-Localy Cooperation Chinese Academy of Sciences, Ningbo Science and Technology Bureau (Grants Nos. 2011C50009, 2011A610140, 2011A610121, and 2010A610159), the CAS/SAFEA International Partnership Program for Creative Research Teams, the aided program for Science and Technology Innovative Research Team of Ningbo Municipality (Grant No. 2009B21005). And the Projects Sponsored by the Scientific Research Foundation for the Returned Overseas Chinese Scholars, State of Ministry of Human Resources & Social Security. Y.L. also thanks Dr. Xiaokun Li, Dr. Leyong Zeng, Dr. Xinmei Zhao, Rui Pang, Lujie Cao, Bo Li, Lijing Miao, Lin Zheng, and Ru Liu for very helpful discussions.

Appendix A. Supplementary data

Supplementary data associated with this article can be found, in the online version, at <http://dx.doi.org/10.1016/j.talanta.2012.03.039>.

References

- [1] G.A. Knauer, J.H. Martin, R.M. Gordon, *Nature* 297 (1982) 49–51.
- [2] M. Kobayashi, S. Shimizu, *Eur. J. Biochem.* 261 (1999) 1–9.
- [3] D.G. Barceloux, D. Barceloux, *Clin. Toxicol.* 37 (1999) 201–206.
- [4] M. Ghaedi, A. Shokrollahi, F. Ahmadi, H.R. Rajabi, M. Soylak, *J. Hazard. Mater.* 150 (2008) 533–540.
- [5] S.R. Yousefi, S.J. Ahmadi, *Microchim. Acta* 172 (2011) 75–82.

- [6] A.I. Stoica, M. Peltea, G.E. Baiulescu, M. Ionica, *J. Pharm. Biomed. Anal.* 36 (2004) 653–656.
- [7] A.I. Yuzefovskiy, R.F. Lonardo, M. Wang, R.G. Michel, *J. Anal. At. Spectrom.* 9 (1994) 1195–1202.
- [8] A.R. Khorrami, A.R. Fakhari, M. Shamsipur, H. Naeimi, *Int. J. Environ. Anal. Chem.* 89 (2009) 319–329.
- [9] S.H. Mashraqui, M. Chandiramani, R. Betkar, K. Poonia, *Tetrahedron Lett.* 51 (2010) 1306–1308.
- [10] N. Shokoufi, F. Shemirani, F. Memarzadeh, *Anal. Chim. Acta* 601 (2007) 204–211.
- [11] D. Badocco, P. Pastore, G. Favaro, C. Maccá, *Talanta* 72 (2007) 249–255.
- [12] S. Zhao, Y. Huang, M. Shi, J. Huang, Y. Liu, *Anal. Biochem.* 393 (2009) 105–110.
- [13] M. Ghaedi, F. Ahmadi, A. Shokrollahi, *J. Hazard. Mater.* 142 (2007) 272–278.
- [14] A. Afkhami, M. Abbasi-Tarighata, H. Khanmohammadi, *Talanta* 77 (2009) 995–1001.
- [15] Y. Yao, D. Tian, H. Li, *Appl. Mater. Interfaces* 2 (2010) 684–690.
- [16] D. Maity, T. Govindaraju, *Inorg. Chem.* 50 (2011) 11282–11284.
- [17] X. Li, J. Wang, L. Sun, Z. Wang, *Chem. Commun.* 46 (2010) 988–990.
- [18] F. Zhang, L. Zeng, C. Yang, J. Xin, H. Wang, A. Wu, *Analyst* 136 (2011) 2825–2830.
- [19] F. Zhang, L. Zeng, Y. Zhang, H. Wang, A. Wu, *Nanoscale* 3 (2011) 2150–2154.
- [20] J. Zhang, X. Xu, Y. Yuan, C. Yang, X. Yang, *Appl. Mater. Interfaces* 3 (2011) 2928–2931.
- [21] Ambient water quality guidelines for cobalt, Section 2(e) of the Environment Management Act (1981) ISBN 0-7726-5228-7.
- [22] X. Liu, Q. Dai, L. Austin, J. Coutts, G. Knowles, J. Zou, H. Chen, Q. Huo, *J. Am. Chem. Soc.* 130 (2008) 2780–2782.
- [23] J.R. Kalluri, T. Arbnesi, S.A. Khan, A. Neely, P. Candice, B. Varisli, M. Washington, S. McAfee, B. Robinson, S. Banerjee, A.K. Singh, D. Senapati, P.C. Ray, *Angew. Chem. Int. Ed.* 48 (2009) 1–5.
- [24] X. Miao, L. Ling, X. Shuai, *Chem. Commun.* 47 (2011) 4192–4194.
- [25] A. Simon, L. MacAleese, P. Maitre, J. Lemaire, T.B. McMahon, *J. Am. Chem. Soc.* 129 (2007) 2829–2840.
- [26] Y. Leng, M. Zhang, C. Song, M. Chen, Z. Lin, *J. Mol. Struct. (THEOCHEM)* 858 (2008) 52–65.
- [27] X. Xu, W. Yu, Z. Huang, Z. Lin, *J. Phys. Chem. B* 114 (2010) 1417–1423.
- [28] D.M. Close, *J. Phys. Chem. A* 115 (2011) 2900–2912.
- [29] N.R. Jana, L. Gearheart, C.J. Murphy, *J. Phys. Chem. B* 105 (2001) 4065–4067.
- [30] A.I. Ermakov, V.V. Belousov, *J. Struct. Chem.* 48 (2007) 6–15.
- [31] S. Bulusu, X. Li, L. Wang, X.C. Zeng, *Proc. Natl. Acad. Sci. U.S.A.* 103 (2006) 8326–8330.
- [32] H. Qian, W.T. Eckenhoff, Y. Zhu, T. Pintauer, R. Jin, *J. Am. Chem. Soc.* 132 (2010) 8280–8281.
- [33] J. Li, X. Li, H. Zhai, L. Wang, *Science* 299 (2003) 864–867.
- [34] J.F. Moulder, W.F. Stickle, P.E. Sobol, K.D. Bomben, J. Chastain (Eds.), *Handbook of X-ray Photoelectron Spectroscopy*, 5th ed., Perkin-Elmer Co., Eden Prairie, 1992.
- [35] <http://www.lasurface.com>.
- [36] R. Wyckoff, *Crystal Structures*, 2nd ed., Wiley Interscience Publishers, Inc, New York, 1963.
- [37] A.A. Athawale, M. Majumdar, H. Singh, K. Navinkiran, *Def. Sci. J.* 60 (2010) 507–513.